Geoderma 357 (2020) 113942

Contents lists available at ScienceDirect

Geoderma

journal homepage: www.elsevier.com/locate/geoderma

Edaphic and microbial determinants of the residence times of active and slow C pools on the Tibetan Plateau

Ding Guo[a,b,*], Xudong Li[a], Jing Wang[a], Decao Niu[a], Wenfei Guo[a], Hua Fu[a,*], Yiqi Luo[c]

[a] State Key Laboratory of Grassland Agro-Ecosystems, Engineering Research Center of Grassland Industry, Ministry of Education, College of Pastoral Agriculture Science and Technology, Lanzhou University, Lanzhou 730000, China
[b] The Key Laboratory of Education Ministry on Environment and Ecology in Tibetan Plateau, Qinghai Normal University, Xining 810028, China
[c] Center for Ecosystem Science and Society, Northern Arizona University, AZ 86011, USA

ARTICLE INFO

Handling Editor: Ingrid Kögel-Knabner

Keywords:
Data assimilation
Decomposition rate
Residence time
Microbial quotient
Soil pH
Soil organic carbon

ABSTRACT

One major source of uncertainties in the estimation of soil organic carbon (SOC) dynamics is carbon (C) residence time, an important parameter in terrestrial ecosystem C cycling models. To better predict terrestrial dynamics, C residence time and its controlling factors need to be well quantified and investigated. In this study, we applied a data assimilation approach to quantify the residence times of different soil C pools on the Tibetan Plateau, based on incubated soil carbon dioxide (CO_2) efflux data. We also assessed the effects of soil properties on C residence times. Our results showed that the residence times of active (RT_A) and slow (RT_S) C pools were well estimated through data assimilation. Soil physical, chemical, and microbial properties significantly regulated RT_A and RT_S. The RT_A was higher in soils with high clay contents ($R^2 = 0.52, p < 0.01$) and low microbial quotients (qMB) ($R^2 = 0.55, p < 0.01$), whereas, the RT_S was higher in soils with high clay contents ($R^2 = 0.76$, $p < 0.01$), high C:N ratios ($R^2 = 0.44$, $p < 0.05$), low qMBvalues ($R^2 = 0.50$, $p < 0.05$), and low soil pH values ($R^2 = 0.80$, $p < 0.01$). Structural equation modeling (SEM) analyses indicated that the model could explain 55% and 91% of the variations in the RT_A and RT_S, respectively. The qMB was the key factor in regulating the RT_A, while soil pH was the crucial variable in controlling the RT_S. These results demonstrated that the major controlling factors on the RT_A and RT_S were different. Considering these variables and their different controls on residence times of different soil C pools could provide more accurate estimation of terrestrial C cycles, and prediction of future C-climate feedbacks.

1. Introduction

Soil organic carbon (SOC) is a critical component of the terrestrial ecosystem carbon (C) cycle (Todd-Brown et al., 2013). SOC dynamics involve the release of CO_2 into the atmosphere and the sequestration of CO_2 from the atmosphere which are associated with the amplification or mitigation of climate change (He et al., 2016). The accurate representation of SOC dynamics is essential for explicitly predicting terrestrial ecosystem C cycle and future C cycling feedbacks to climate change (Luo et al., 2016; Todd-Brown et al., 2013, 2014). However, based on the estimation of earth system models (ESMs), there are considerable uncertainties in the prediction of SOC dynamics (Todd-Brown et al., 2013, 2014). For instance, Todd-Brown et al. (2014) estimated changes in global SOC storage over the 21st century which ranged from losses of 72 Pg C to gains of 253 Pg C. Such significant uncertainties are mostly due to indeterminant C residence times (Luo et al., 2016; Todd-Brown et al., 2013). The C residence time is a key indicator for ecosystem functionality and an important parameter in ESMs for determining C storage capacities (Chen et al., 2015). Therefore, the quantification of uncertainties in C residence times is a prerequisite for assessing terrestrial C cycles and predicting future C-climate feedbacks (Anav et al., 2013; Wang et al., 2018).

Soil organic C is heterogeneous and consists of a complex of myriad materials with different residence times, which can range from minutes to millennia (Trumbore, 1997). In the most conventional models, SOC is typically categorized as having at least three C pools (active, slow, and passive) according to its residence time (Parton et al., 1987; Xu et al., 2006). Several methods have been applied for the determination of C residence times, such as C stable isotopes (Derrien and Amelung, 2011), radiocarbon dating (He et al., 2016), and the C balance method (Wang et al., 2018). However, these methods have their limitations. For example, the C stable isotope method may only be applied to

* Corresponding authors at: College of Pastoral Agriculture Science and Technology, Lanzhou University, 768 West Jiayuguan Road, Lanzhou, Gansu 730020, China.
E-mail addresses: guod@lzu.edu.cn (D. Guo), fuhua@lzu.edu.cn (H. Fu).

https://doi.org/10.1016/j.geoderma.2019.113942
Received 23 June 2019; Received in revised form 28 August 2019; Accepted 28 August 2019
Available online 07 September 2019

ecosystems in which dominant plant species are transformed between C_3 and C_4 plants (Derrien and Amelung, 2011). Therefore, uncertainties in residence times of different soil C pools have not been well quantified, which limits our understanding of terrestrial C dynamics and climate-C feedbacks.

The data assimilation approach can optimize parameter estimations by combining observed data with models (Luo et al., 2009). Recently, data assimilation has been employed to estimate the residence times of different C pools (Guo et al., 2017; Xu et al., 2006; Zhou et al., 2012). For instance, Zhang et al. (2010) used data assimilation to estimate the residence times of different C pools among three different forest ecosystems. Schädel et al. (2013) initially applied data assimilation approach to estimate the residence times of different C pools based on soil CO_2 efflux data from soil incubation studies. Data from soil incubation studies contain quantitative information on the residence times of different soil C pools, as there is generally no new input substrate during incubation (Schädel et al., 2014). Moreover, the water content and temperature of soil can be controlled in the incubation studies, and the effects of soil moisture and temperature on the residence times of different C pools can be isolated. This reduces the bias of the relationship between soil properties and the residence times of different C pools, thus, increasing the comparability among different study sites (Holland et al., 2000; Schädel et al., 2013; Schädel et al., 2014).

The Tibetan Plateau is often referred to as the "third pole", due to its frigid temperature. The decomposition of SOC is very slow (i.e. the C residence time is long), which consequently results in the accumulation of large amounts of C in the soil (Yu et al., 2017). The Tibetan Plateau is also one of the most sensitive and vulnerable regions to global climate change, and experiences more rapid warming than other regions (Liu and Chen, 2000; Yu et al., 2017). Consequently, much research has focused on the SOC of the Tibetan Plateau, but these studies to date mostly focus on the spatial distribution and temporal dynamics of SOC storage and controlling factors (Ding et al., 2016a; Wang et al., 2002; Yang et al., 2008). Very few studies have involved soil C residence time (Yu et al., 2017; Zhao et al., 2015). Moreover, the residence times of different soil C pools and their controlling factors have not been reported in this region. In this study, we measured the physical, chemical and microbial properties of soils, and applied a data assimilation approach to quantify the residence times of different soil C pools, based on time series data from long term soil incubation studies. The aims of this investigation were to: (1) quantify the residence times of different soil C pools; (2) evaluate the relationships between soil C residence times and soil properties; and (3) identify the controlling factors for soil C residence times.

2. Materials and methods

2.1. Site description and sampling

The research area is located in the Tibetan Autonomous Prefecture of Haibei in Qinghai Province, with a typical continental alpine climate. Soils were collected at four sites, including two alpine steppes (AS-E and AS-S), one alpine meadow (AM), and one alpine swamp meadow (ASM), were sampled in August 2016. The soils were classified as Cambisols at the AS-E, AS-S and AM sites, and Gleysols at the ASM site (Baumann et al., 2009; Chen et al., 2016a; Yang et al., 2015) according to the Food and Agriculture Organization classification scheme (FAO, 2006). The details of the four sites are described in Table 1. Four $50 \times 50\ m^2$ replicate plots, approximately 50 m apart, were randomly selected at each sampling site. In each plot, soil samples were collected from five sampling points at depth of 0–10, 10–20, and 20–30 cm, which were subsequently mixed as single samples to represent each depth. The soil samples were immediately sieved to < 2 mm to remove any roots and stones following collection and transported to the laboratory in an icebox. One portion of the sieved soil sample was stored at 4 °C for microbial biomass measurements and laboratory incubation, whereas the other portion was air-dried for physical and chemical analyses.

2.2. Soil analysis

Soil water content (SWC) was measured by oven drying the samples at 105 °C. Soil bulk density (BD) was measured using a known volume ring (100 cm^3) method. Soil texture was determined using a Mastersizer 2000 laser particle size analyzer (Malvern, Worcestershire, UK). Soil pH was determined in a 1:2.5 (w/v) soil/water ratio with a pH meter (PHS-3C, INESA, Shanghai, China). Soil organic carbon (SOC) was determined via a potassium dichromate oxidation method (Nelson and Sommers, 1996). Soil total nitrogen (TN) concentration was quantified using the Kjeldahl method (Bremner, 1996).

The light fraction of soil organic carbon (LF-OC) was extracted using a 1.7 g ml^{-1} NaI solution (Gregorich and Beare, 2008). Briefly, 10 g of the air-dried soil sample was introduced into a centrifuge tube with a 20 ml NaI solution. After agitating for 60 min and standing for 48 h, the supernatant was filtered using 0.45 μm filter. The light fraction was rinsed with 0.01 M $CaCl_2$ and distilled water, and then dried at 60 °C for 48 h to obtain the final weight. The light fraction was then ground to pass through 0.25 mm sieve, after which the concentration of C was determined. The LF-OC was calculated as the C concentration in the light fraction multiplied by the total mass of light fraction.

Soil C mineralization was determined by the alkaline absorption method using laboratory incubation (Alef, 1995). Fresh soil samples (60 g) were modified to 60% water holding capacity, and incubated in l L mason jars at 25 °C. The CO_2 released from soil was trapped in 10 ml 0.5 M NaOH within mason jars, and measured by titration with 0.1 M HCl at 4, 8, 12, 16, 20, 27, 34, 41, 48, 55, 62, 69, 76, 90, 104, 118, 132, 162, 192, 222, 252, 282, 312, 342 and 372 days. Simultaneously, four mason jars containing NaOH vials without soil samples were used as controls.

Soil microbial biomass C and N (SMBC and SMBN) were determined through a fumigation-extraction method (Brookes et al., 1985; Vance et al., 1987). The fumigated and non-fumigated soil samples were extracted using 0.5 M K_2SO_4 (1:4 (w/v) soil: extractant). The organic C and N in the extracts were measured using a Vario TOC analyzer (Elementar, Langenselbold, Germany). The SMBC and SMBN were calculated as the differences in the C and N content between in the fumigated and non-fumigated soil samples, using the conversion factors of 0.45 and 0.54, respectively. The microbial quotient (qMB) was calculated as the ratio of SMBC and SOC (SMBC/SOC, %). The microbial metabolic quotient (qCO_2) was calculated as the ratio of basal respiration and SMBC (mg CO_2-C g^{-1} SMBC day^{-1}).

2.3. Model description

Soil organic C is comprised of continuous materials with different turnover rates, ranging from days to millennia, which is typically represented by models with multiple C pools (Trumbore, 1997). A three-pool C decomposition model (Guo et al., 2017), consisting of active, slow and passive pools was employed for this study (Eq. (1)).

$$R_t = \sum_{i=1}^{3} A_i C (1 - e^{-k_i t}) \quad (1)$$

where R_t is the cumulative CO_2-C efflux after time t (mg C g^{-1} soil). A_i (i = 1, 2, 3) describes the initial partitioning coefficient of active, slow and passive SOC (%), respectively, and $A_1 + A_2 + A_3 = 1$. C is the initial SOC content (mg C g^{-1} soil). K_i denotes the decomposition rates of ith C pool. The parameters A_i and K_i were the targets to be determined. The inverses of the parameter K_i are the C residence times of different soil C pools.

Table 1
The four study site characteristics description.

Site	Ecosystem types	Latitude (N)	Longitude (E)	Altitude (m)	MAP (mm)	MAT (°C)	Dominate species	Coverage (%)	Biomass (g m^{-2})
AS-E	Alpine steppe	37°37′	101°19′	3200	561	−1.7	*Elymus nutans Griseb.*	90 a	422.81 c
AS-S	Alpine steppe	37°57′	101°51′	3133	405	0.94	*Stipa capillata Linn.*	86 a	349.12 c
AM	Alpine meadow	37°44′	101°05′	3748	420	−3.3	*Kobresia humilis*	93 a	524.91 b
ASM	Alpine swamp meadow	36°42′	100°47′	3210	433	−0.7	*Kobresia tibetica*	89 a	781.72 a

Different letter means significant difference among different sites, values indicate mean.

2.4. Data assimilation

For this study, a Bayesian probabilistic inversion approach (Eq. (2)) was used to optimize the partitioning coefficient and decay rate of the C decomposition model (Xu et al., 2006).

$$p(\theta \mid Z) \propto p(Z \mid \theta)p(\theta) \tag{2}$$

where the posterior probability density function (PDF) $p(\theta|Z)$ of parameters may be obtained from prior knowledge of the parameters represented by prior PDF $p(\theta)$ and the information contained in the SOC mineralization data was represented by a likelihood function $p(Z|\theta)$. The prior PDF $p(\theta)$ was specified by giving specific parameter ranges (Chen et al., 2016b; Guo et al., 2017; Xu et al., 2006; Xu et al., 2016) with uniform distribution (Table 2). The likelihood function $p(Z|\theta)$ was calculated on the basis of the assumption that errors between the observed and modeled data were independently distributed.

$$p(Z \mid \theta) \propto exp\left\{-\frac{1}{2\sigma^2}\sum_{t\in obs(Z_i)}[Z_i(t) - X_i(t)]^2\right\} \tag{3}$$

where Z_i(t) and X_i(t) are the observed and modeled cumulative SOC mineralized values, and σ^2 is the standard deviation of cumulative SOC mineralized values.

The Metropolis-Hastings (M-H) algorithm was used to construct the posterior PDF of parameters, which is a Markov Chain Monte Carlo (MCMC) technique (Hastings, 1970; Metropolis et al., 1953). The M-H algorithm repeats two steps: a proposing step and a moving step (Xu et al., 2006). In the proposing step, a new parameter point θ^{new} is generated on the basis of a previously accepted parameter point θ^{old} with a proposal distribution $p(\theta^{new}|\theta^{old})$.

$$\theta^{new} = \theta^{old} + r(\theta_{max} - \theta_{min})/D \tag{4}$$

where θ_{min} and θ_{max} are the minimum and maximum of given parameter values in the prior range. r is a random variable between −0.5 and 0.5 with a uniform distribution, and D is set to 10 to control the proposing step size. In the moving step, the new parameter θ_{new} is tested against the Metropolis criterion to examine if it should be accepted or rejected. The M-H algorithm was run 4 replicates and 100,000 times for each replicate to facilitate extraction of soil C incubation data.

Table 2
Prior ranges of parameters for the C dynamics model.

Parameters	Description	Unit	Intervals
A_1	Partitioning coefficient of active C pool	%	0–9[a]
A_2	Partitioning coefficient of slow C pool	%	30–80
K_1	Decay rates of active C pool	day^{-1}	0–0.05
K_2	Decay rates of slow C pool	day^{-1}	0–2e−3[a]
K_3	Decay rates of passive C pool	day^{-1}	0–9e−5

A_i: partitioning coefficient of different C pool, K_i: decomposition rate of different C pool.

[a] In soil at AM site, the prior ranges of A_1 was set to 0–5%, the prior ranges of K_2 was set to 0–1e−3.

2.5. Data analysis

One-way analysis of variance (ANOVA) was employed to compare soil C mineralization and soil physical (SWC, BD, and clay content), chemical (pH, SOC, TN, C:N and LF-OC), and microbial (SMBC, SMBN, qMB, SMBC:SMBN and qCO_2) properties between the four study sites at the same soil layer. The accepted parameters were used to simulate cumulative CO_2-C release using Eq. (1). We conducted regression analysis to explore the relationships between modeled and observed cumulative CO_2-C release. The coefficient of determination (R^2) and root mean squared error (RMSE, Eq. (5)) were estimated to assess goodness of fit. Regression analysis was also performed to determine the relationships between the residence times of active and slow C pools, and soil physical, chemical and microbial properties, as well as the relationships between soil pH and microbial properties. We performed structure equation modeling (SEM) to determine the relative impacts of soil physical, chemical and microbial properties on the residence times for the different soil C pools. Variables that were significantly correlated with the residence times of different C pools were included in SEM analyses (Chen et al., 2016b; Ding et al., 2016b). The SEM analyses were performed using AMOS 21.0 (SPSS Inc., Chicago, IL, USA). All other data analyses were conducted with SPSS 17.0 for Windows (SPSS, Inc., Chicago, IL, USA).

$$RMSE = \sqrt{\frac{1}{n}\sum_{t=1}^{n}(Z_t - X_t)^2} \tag{5}$$

where n is the number of measurement points (i.e. n = 25), and Z_t and X_t are the observed and modeled cumulative SOC mineralized values at t times.

3. Results

3.1. Soil properties

The SWC were generally higher at the AM and ASM sites than that at the AS-E and AS-S sites ($p < 0.05$, Table 3). The SWC was significantly different between the AS-E and AS-S sites in 0–10 cm soil layer, and between the AM and ASM site in 0–20 cm soil layers ($p < 0.05$). Soil BD was higher at the AS-E and AS-S sites compared to that at the AM and ASM sites in all soil depths. Significant differences were found for soil BD between the AS-E and AS-S site in 10–30 cm soil layers, and between the AM and ASM site in 0–20 cm soil layers ($p < 0.05$). Clay contents were the highest at the AM site (10.7%–11.79%), followed by that at the AS-E (8.82%–10.47%) and AS-S (7.01%–8.22%) sites, and the lowest at the ASM (4.42%–5.63%) sites.

The highest pH was found at the ASM (8.26–8.4) site, followed by that at the AS-E (7.95–8.08) and AS-S (7.88–8.11) sites, and the lowest at the AM (6.68–6.91) site (Table 3). SOC was the highest at the AM site and the lowest at the AS-S site. A similar trend was found for TN. The C:N ratio was higher at the AM site than that at the AS-E and AS-S sites ($p < 0.05$), whereas no significant differences were observed among AS-E, AS-S and ASM sites. The LF-OC varied from 4.95 g kg^{-1} soil to 63.93 g kg^{-1} soil at four sites. Compared with AS-E and AS-S sites, LF-OC was higher at the AM and ASM site. Significant differences in the LF-OC were detected between AS-E and AS-S sites in 10–20 cm soil layer,

Table 3
Soil physical, chemical and microbial properties for the experiment sites.

Depth (cm)	Site	SWC	BD	Clay	pH	SOC
0–10	AS-E	38.65 ± 4.89 c	0.94 ± 0.07 a	8.82 ± 0.44 b	7.95 ± 0.05 b	76.78 ± 4.82 b
	AS-S	23.05 ± 2.87 d	0.96 ± 0.02 a	8.05 ± 0.44 c	7.88 ± 0.06 b	52.77 ± 2.80 c
	AM	110.87 ± 7.94 a	0.51 ± 0.03 c	10.70 ± 0.53 a	6.91 ± 0.03 c	194.70 ± 14.49 a
	ASM	73.71 ± 4.59 b	0.66 ± 0.07 b	5.04 ± 0.25 d	8.40 ± 0.07 a	73.25 ± 1.90 b
10–20	AS-E	25.83 ± 2.20 c	1.16 ± 0.06 a	9.48 ± 0.70 b	8.02 ± 0.01 b	45.88 ± 1.85 b
	AS-S	20.16 ± 1.77 c	1.04 ± 0.04 b	8.22 ± 0.28 c	7.92 ± 0.09 c	43.36 ± 2.76 b
	AM	102.56 ± 7.66 a	0.59 ± 0.02 d	11.44 ± 0.23 a	6.68 ± 0.03 d	138.14 ± 12.72 a
	ASM	83.24 ± 7.32 b	0.73 ± 0.05 c	4.42 ± 0.36 d	8.26 ± 0.04 a	49.95 ± 2.98 b
20–30	AS-E	26.47 ± 0.86 b	1.16 ± 0.08 a	10.47 ± 0.28 b	8.08 ± 0.04 b	37.14 ± 2.96 bc
	AS-S	18.17 ± 1.51 b	1.06 ± 0.03 b	7.01 ± 0.17 c	8.11 ± 0.04 b	31.21 ± 1.20 c
	AM	89.47 ± 9.50 a	0.85 ± 0.03 c	11.79 ± 0.33 a	6.77 ± 0.04 c	95.84 ± 8.91 a
	ASM	81.01 ± 11.33 a	0.84 ± 0.03 c	5.63 ± 0.47 ± d	8.39 ± 0.03 a	42.05 ± 5.82 b

Depth (cm)	TN	C:N	LF-OC	SMBC	SBMN	qMB	SMBC:SMBN	qCO_2
0–10	6.01 ± 0.51 b	12.79 ± 0.30 b	18.48 ± 2.18 c	683.82 ± 32.96 c	172.88 ± 7.39 a	0.89 ± 0.03 d	3.96 ± 0.10 d	86.41 ± 7.74 a
	4.26 ± 0.23 c	12.39 ± 0.47 b	19.23 ± 1.28 c	840.11 ± 62.29 c	118.57 ± 11.29 c	1.60 ± 0.17 b	7.10 ± 0.37 c	63.36 ± 7.28 b
	13.98 ± 1.33 a	13.96 ± 0.76 a	63.93 ± 4.81 a	2443.19 ± 247.68 a	140.34 ± 20.67 b	1.26 ± 0.11 c	17.52 ± 1.33 b	39.03 ± 4.07 c
	5.64 ± 0.50 b	13.06 ± 0.99 ab	36.30 ± 6.99 b	1805.72 ± 150.79 b	87.70 ± 7.76 d	2.47 ± 0.23 a	20.64 ± 1.45 a	57.97 ± 5.26 b
10–20	3.83 ± 0.23 c	11.74 ± 0.39 b	7.79 ± 0.51 d	366.79 ± 21.94 b	72.65 ± 9.17 b	0.82 ± 0.03 b	5.09 ± 0.54 b	63.09 ± 4.17 b
	3.61 ± 0.10 c	12.02 ± 0.58 b	13.53 ± 2.01 c	386.51 ± 39.41 b	99.37 ± 8.24 a	0.90 ± 0.14 b	3.91 0.51 b	61.61 ± 9.26 b
	9.79 ± 0.34 a	14.10 ± 0.89 a	34.52 ± 3.65 a	725.26 ± 65.87 a	71.70 ± 13.42 b	0.53 ± 0.10 c	10.38 ± 2.10 a	52.01 ± 7.73 b
	4.77 ± 0.41 b	10.57 ± 1.6 b	20.89 ± 1.54 b	796.17 ± 63.00 a	77.11 ± 7.47 b	1.60 ± 0.20 a	10.39 ± 1.20 a	79.51 ± 8.68 a
20–30	3.19 ± 0.25 b	11.67 ± 0.73 b	5.07 ± 1.36 b	225.23 ± 28.75 c	53.97 ± 6.32 a	0.60 ± 0.06 bc	4.26 ± 1.08 b	68.24 ± 5.63 a
	2.73 ± 0.21 b	11.44 ± 0.50 b	4.95 ± 1.17 b	199.59 ± 38.64 c	54.01 ± 10.79 a	0.64 ± 0.13 b	3.73 ± 0.56 b	60.95 ± 15.58 a
	6.70 ± 1.08 a	14.51 ± 2.13 a	13.70 ± 3.83 a	365.38 ± 48.24 b	48.73 ± 6.70 a	0.39 ± 0.07 c	7.53 ± 0.68 a	64.76 ± 11.57 a
	3.33 ± 0.33 b	12.71 ± 2.01 ab	17.22 ± 4.33 a	475.23 ± 53.11 a	60.22 ± 6.08 a	1.15 ± 0.25 a	7.96 ± 1.30 a	80.88 ± 5.24 a

SWC, soil water content (%), BD, bulk density ($g\,cm^{-3}$), SOC, soil organic carbon ($g\,kg^{-1}$ soil), TN, total nitrogen ($g\,kg^{-1}$ soil), C:N, SOC:TN, LF-OC ($g\,kg^{-1}$), SOC content of light fraction, SMBC, soil microbial biomass carbon ($mg\,kg^{-1}$), SMBN, soil microbial biomass nitrogen ($mg\,kg^{-1}$), qMB, microbial quotient (%), qCO_2, microbial metabolic quotient (mg CO_2-C g^{-1} SMBC day^{-1}). Different letter means significant difference among different sites in the same soil depths, values indicate mean ± SD.

and between AM and ASM sites in 0–20 cm soil layers (Table 3).

In the 0–30 cm soil layers, higher SMBC were observed at the AM and ASM sites than those at the AS-E and AS-S sites (Table 3). There were no significant differences in SMBC between AS-E and AS-S in 0–30 cm soil layers, whereas significant differences in SMBC between AM and ASM were found in the 0–10 cm and 20–30 cm soil layers. In the 0–10 cm soil layer, SMBN significantly decreased in the order as follow: AS-E > AM > AS-S > ASM. The SMBN was significantly higher at the AS-S than that at the AS-E, AM and ASM sites in the 10–20 cm soil layer. There was no significant difference among the four study sites in the 20–30 cm soil layer. The highest qMB were observed at the ASM site, followed by that at the AS-E and AS-S sites, and the lowest at the ASM site except that in the 0–10 cm soil layer. The SMBC:SMBN were higher at the AM and ASM sites than those at the AS-E and AS-S sites in all soil depths, whereas significant differences in SMBC:SMBN were found between AS-E and AS-S sites, and between AM and ASM sites only in the 0–10 cm soil layer. The highest qCO_2 was observed at the AS-E site, followed by AS-S and ASM sites, and the lowest at the AM site in the 0–10 cm soil layer. In the 10–20 cm soil layer, the qCO_2 was higher at the ASM than that at the other sites. No significant differences were found among the vegetation types in 20–30 cm soil layer (Table 3).

3.2. Soil C mineralization

The C mineralization rate patterns of the soil samples over time were similar across all vegetation types, which were initially high, but declined rapidly at the early stage and leveled off as the incubation processed (Fig. 1), indicating that the contribution of labile C pool dominated the C mineralization at the early stage, while the recalcitrant C pool dominated C mineralization at the later stage. Moreover, our inverse analysis results directly demonstrated that the active C pool contributed for 76%–79% to the C mineralization rate at the beginning of the incubation. The slow C pool dominated C mineralization after 104 days, 118 days and 62 days incubation at the AS-E and AS-S sites, at the AM site and at the ASM site, respectively (Table S1). Over the

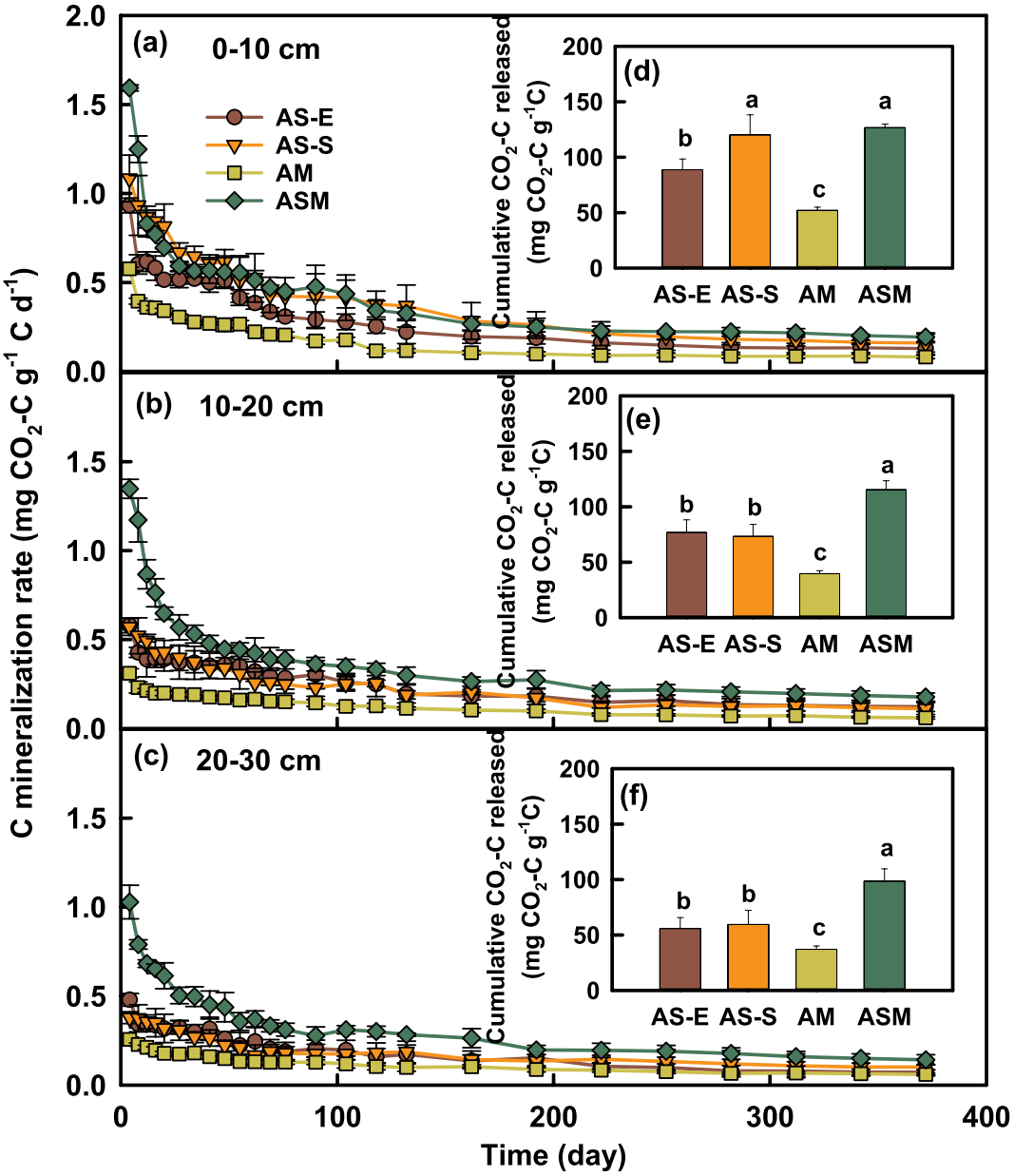

Fig. 1. Carbon mineralization rate (a–c) and cumulative CO_2-C released (d–f) at three soil depths over the 372 days incubation experiment. Values are means ± SE, n = 4.

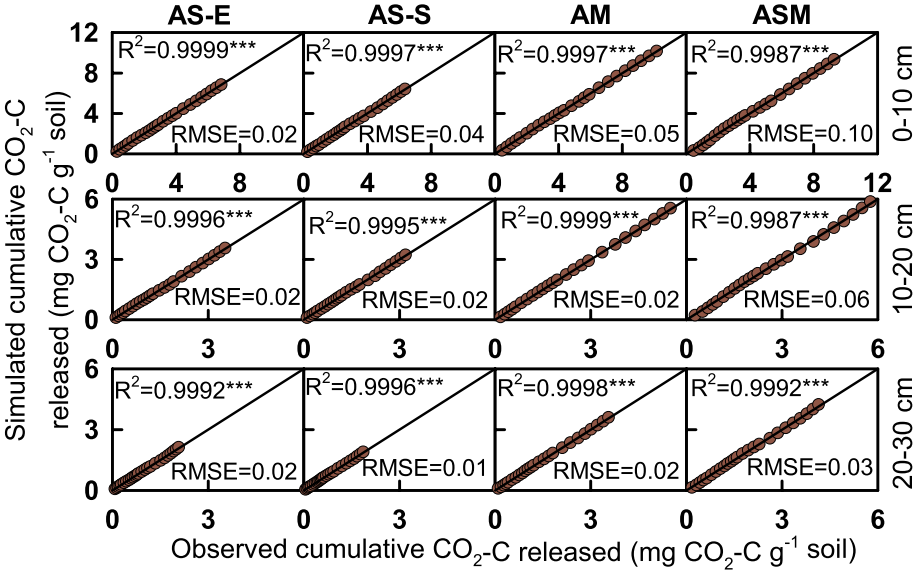

Fig. 2. Relationship between modeled and observed cumulative release of CO_2-C. RMSE, root mean squared error. *$p < 0.05$, **$p < 0.01$, ***$p < 0.001$.

372 days incubation experiment, the cumulative CO_2-C release ranged from 40.80 to 126.74 mg CO_2-C g^{-1} SOC. The highest cumulative CO_2-C release was observed from ASM (126.74 mg CO_2-C g^{-1} SOC) and AS-S (120.28 mg CO_2-C g^{-1} SOC), while the lowest value was recorded at the AM site (52.15 mg CO_2-C g^{-1} SOC) in the 0–10 cm soil layer ($p < 0.05$, Fig. 1d). The quantity of cumulatively released CO_2-C diminished significantly ($p < 0.05$) in the order: ASM > AS-E and AS-S > AM in the 10–30 cm soil layers (Fig. 1e and f).

3.3. Data assimilation of soil C dynamics

The observed and simulated cumulatively released CO_2-C fitted well ($R^2 > 0.99$, $p < 0.001$, RMSE < 0.10, Fig. 2), which indicated that the three pool C decomposition model performed well. According to the results of the data assimilation, the partitioning rate of the active C pool (A_1), and the decay rate of the active (K_1) and slow (K_2) C pools were nearly Gaussian distributed, suggesting that the A_1, K_1 and K_2 parameters were well constrained (Fig. 3). However, the partitioning rate of the slow C pool (A_2) and decay rate of the passive C pool (K_3)

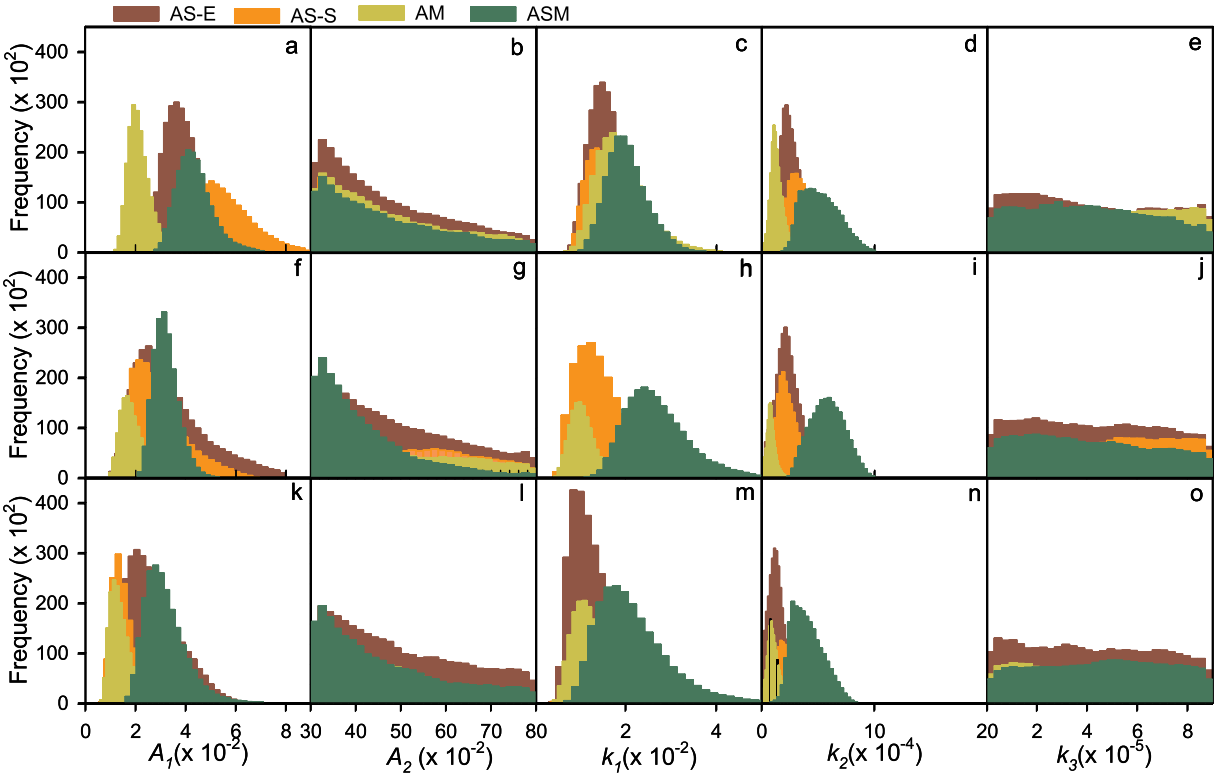

Fig. 3. Frequency distribution of the posterior PDF of the parameters at three soil depths: 0–10 cm (a–e), 10–20 cm (f–j) and 20–30 cm (k–o). A_i: partitioning coefficient of different C pools, K_i: decay rate of different C pools.

Table 4
The maximum likelihood estimates (MLE) or mean of parameters for the C dynamics model.

Depth (cm)	Site	A_1 (%)	A_2 (%)	$K_1 \times 10^{-2}$ (day^{-1})	$K_2 \times 10^{-4}$ (day^{-1})	$K_3 \times 10^{-5}$ (day^{-1})	$1/K_1$ (day)	$1/K_2$ (year)	$1/K_3$ (year)
0–10	AS-E	3.64	47.05	1.48	2.19	4.22	67.57	12.51	64.92
	AS-S	5.05	46.95	1.37	3.11	4.45	72.99	8.81	61.59
	AM	1.92	47.10	1.71	1.07	4.92	58.48	25.60	55.68
	ASM	4.11	46.77	2.41	5.96	4.14	41.49	4.60	66.1
10–20	AS-E	2.52	48.57	0.875	2.11	4.29	114.29	12.98	63.90
	AS-S	2.16	48.06	1.24	1.95	4.75	80.65	14.05	57.63
	AM	1.67	50.99	0.982	0.731	4.08	101.83	37.48	67.19
	ASM	3.13	41.83	1.95	4.31	4.08	51.28	6.36	67.17
20–30	AS-E	2.05	49.76	0.847	1.14	4.27	118.06	24.03	64.09
	AS-S	1.32	45.64	1.38	1.74	4.27	72.46	15.75	64.12
	AM	1.13	45.95	1.09	0.768	3.98	91.74	35.67	68.79
	ASM	2.79	46.39	1.79	2.75	4.57	55.87	9.96	59.95

A_i: partitioning coefficient of different C pool, K_i: decomposition rate of different C pool.

parameters were not constrained, which was likely the results of limited data for calibration. Only a small proportion of the released CO_2-C was derived from the passive C pool, which made it difficult to estimate its decay rate. Maximum likelihood estimates were calculated for the well constrained parameters (A_1, K_1 and K_2), and the mean values were calculated for the non-constrained parameters (A_2 and K_3).

Our results revealed that the parameters A_1, A_2 and A_3 were different between vegetation types, ranging between 1.13% and 5.05%, 41.83% and 50.99%, and 47.37% and 55.04%, respectively (Table 4). The mean parameters A_1, A_2 and A_3 for the three soil depths was the highest at the ASM site (3.34%), the AS-E site (48.46%) and the ASM site (51.66%), respectively, and the lowest at the AM site (1.57%), the ASM site (45.00%) and the AS-E site (48.80%), respectively. The residence times of the active (RT_A) slow (RT_S) and passive (RT_P) C pools ranged from 41 and 118 days, 5 and 37 years, and 56 and 69 years, respectively (Table 4). The ASM site exhibited the lowest RT_A across all soil depths, while the AS-S and AS-E sites showed the highest RT_A for the 0–10 cm and 10–30 cm soil depths, respectively. The RT_S were the highest at the AM site (26 to 37 years), followed by the AS-E (13 to 24 years) and AS-S site (9 to 16 years), with the lowest value at the ASM site (5 to 10 years). The RT_P was highest in ASM site and lowest in AM site in the 0–10 cm soil layer. The AM site had the highest RT_P in the 10–30 cm soil layers, while the lowest RT_P in the 10–20 and 20–30 cm soil layers was in AS-S and ASM sites, respectively.

3.4. Linking soil C residence time to physical, chemical and microbial properties

Based on the data assimilation results, we analyzed the linear relationships between the well constrained residence time (RT_A and RT_S) and soil properties. Linear regression analyses indicated that the RT_A and RT_S were significantly associated with soil physical, chemical, and microbial properties (Fig. 4). The RT_A was significantly positively correlated with the clay content ($R^2 = 0.52$, $p < 0.01$; Fig. 4c) and negatively correlated with qMB ($R^2 = 0.55$, $p < 0.01$; Fig. 4i). The RT_A was not significantly affected by the other soil physical, chemical and microbial properties measured in this study (Fig. 4). The RT_S significantly increased with the clay content ($R^2 = 0.76$, $p < 0.01$) and C:N ratio ($R^2 = 0.44$, $p < 0.05$) but significantly declined with soil pH ($R^2 = 0.80$, $p < 0.01$) and qMB ($R^2 = 0.50$, $p < 0.05$).

The SEM analyses showed that our model explained 55% and 91% of the variations in the RT_A and RT_S, respectively (Fig. 5). The qMB had direct negative effects on the RT_A and RT_S whereas the clay content had

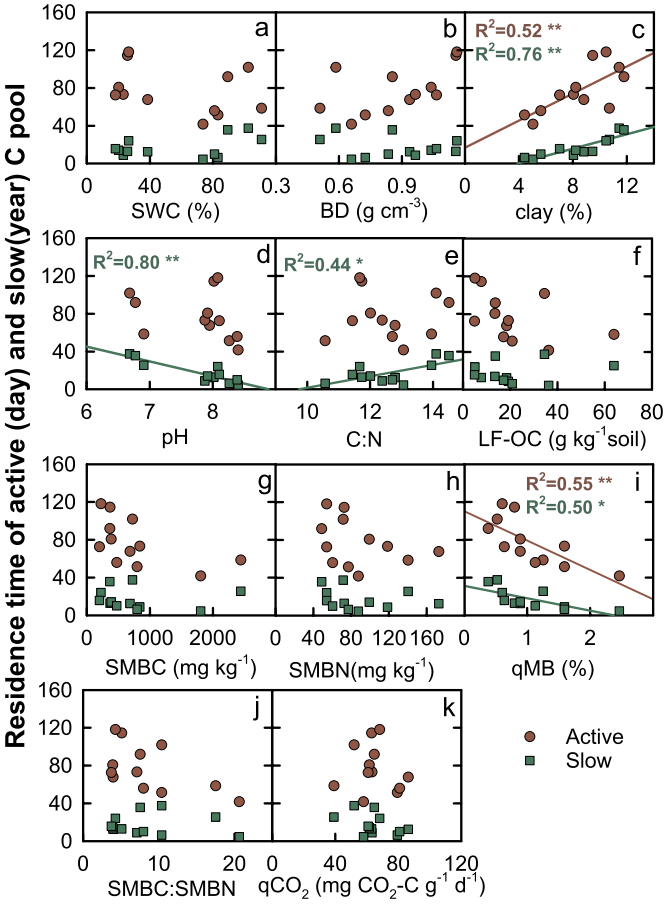

Fig. 4. Relationship between the residence time of active (dark red solid circles) and slow C pool (dark green solid squares) with soil physical (SWC, BD and clay), chemical (pH, C:N, and LF-OC), and microbial (SMBC, SMBN, qMB, SMBC:SMBN and qCO_2) properties. SWC, soil water content; BD, bulk density; LF-OC, light fraction of soil organic carbon; SMBC, soil microbial biomass carbon; SMBN, soil microbial biomass nitrogen; qMB, microbial quotient, the ratio of SMBC to soil organic carbon; qCO_2, microbial metabolic quotient, the ratio of basal respiration rate to SMBC. *$p < 0.05$, **$p < 0.01$. (For interpretation of the references to colour in this figure legend, the reader is referred to the web version of this article.)

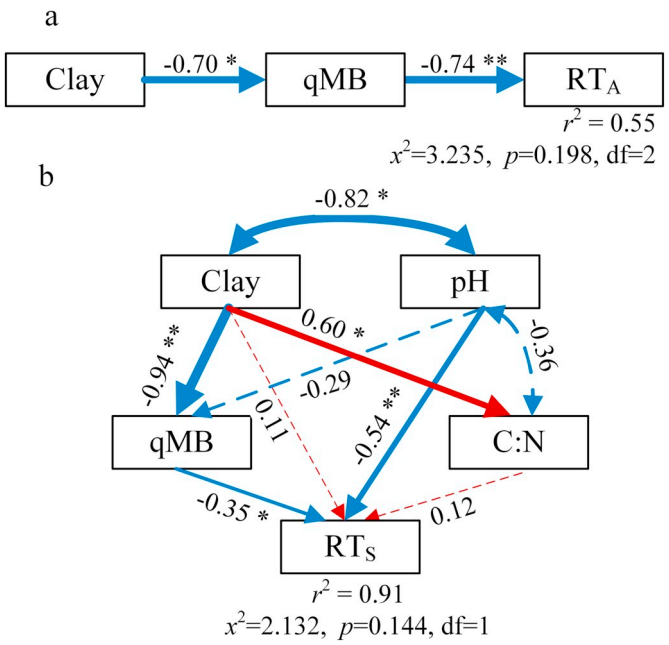

Fig. 5. Structural equation modeling (SEM) examining the direct and indirect effects on the residence times of active (RT_A, a) and slow (RT_S, b) C pools. Solid and dashed arrows indicate significant ($p < 0.05$) and non-significant ($p > 0.05$) effects. Red and blue arrows represent positive and negative effects, respectively. The arrow widths are proportional to the strength of the relationship. qMB, microbial quotient. (For interpretation of the references to colour in this figure legend, the reader is referred to the web version of this article.)

strong indirect effects on the RT_A and RT_S through its negative correlation with qMB. Compared to the standardized path coefficients for residence time, the direct effect of the qMB decreased from −0.74 on the RT_A to −0.35 on the RT_S, and the indirect effect of the clay content decreased from 0.52 on the RT_A to 0.33 on the RT_S. Moreover, soil pH only had consistent direct negative effects on the RT_S (Fig. 5b).

4. Discussion

Numerous previous studies have focused on the residence times (i.e. the inverse of decomposition rate) of different C pools and their controlling factors, and demonstrated that various soil properties (including physical, chemical and microbial properties) regulated the residence times of different C pools (Mtambanengwe et al., 2004; Schädel et al., 2013; Wang et al., 2003; Xu et al., 2016). However, most of those studies separated the SOC into different pools primarily based on physical or chemical fractionations, which were not consistent with the classification of conceptual models. Thus, these methods limited our capacity to understand terrestrial C dynamics and predict climate-C feedbacks. Our data assimilation approach separated the SOC into different pools based on the classification of conceptual model. Therefore, investigations of their control factors are essential to predict C-climate feedbacks.

4.1. Effect of qMB on C residence time

The qMB, which can be interpreted as the availability of soil C to decomposers and the proportion of soil C immobilized within microbial cells (Sparling, 1992), is a more sensitive parameter in revealing microbial activities than SMBC measured alone (Arai et al., 2014; Deng et al., 2016; Serna-Chavez et al., 2013). Therefore, the qMB can be employed as an important index for the decomposition of SOC and may reflect the stabilization of soil C (Landgraf and Klose, 2002; Landgraf et al., 2005; Liao et al., 2011). Our results illustrated that the C residence times increased significantly with decreasing qMB ($p < 0.05$, Fig. 4i), and were directly influenced by the qMB (Fig. 5), which was in line with the previous studies (Landgraf et al., 2005; Liao et al., 2011; Wen et al., 2014). Larger qMB could indicate that soil microbes were more efficient for converting SOC into SMBC, suggesting higher substrate quality for soil microorganisms whereas lower qMB signified a decrease in the availability of substrate (Pajares et al., 2009; Wang et al., 2009; Wei et al., 2011; Wen et al., 2014). Our results also showed that the qMB were positively correlated with the LF-OC:SOC ratio and active C pool size (A_1) ($p < 0.05$, Fig. S1), suggesting that higher soil quality was associated with larger qMB. Furthermore, the increased qMB indicated an increase in microbial functional diversity (Lagomarsino et al., 2011), and thus result in the increase in decomposition of SOC. In addition, the decrease in qMB was significantly correlated with the reduction in fungal:bacterial ratio (Liu et al., 2012). The decreasing proportion of fungi would reduce the decomposition of recalcitrant substrates (Paterson et al., 2008). Consequently, the qMB was positively correlated with the decomposition of active and slow C pool.

4.2. Effect of clay content on C residence time

Soil clay is an important factor regulating SOC decomposition, storage, and stabilization (Oades, 1988; Six et al., 2002; Wagner et al., 2007). Therefore, it has been included in several simulation models as a key element for the control of soil C dynamics (Parton et al., 1987; Percival et al., 2000). It is generally accepted that the SOC decomposition rate is reduced as the clay content increases (i.e. SOC residence time increases with higher clay content) (Giardina et al., 2001; Xu et al., 2016). Consistent with other studies, our results also showed that there was a positive relationship between the clay content and SOC residence time ($p < 0.01$, Fig. 4c).

Two core mechanisms have been proposed to illustrate the effect of soil clay content on the SOC decomposition rate, including chemical and physical protection (Plante et al., 2006; Six et al., 2002; Wagner et al., 2007). First, soil clay particles are anticipated to promote the adsorption of soil organic matter and even the relevant enzymes, and to form organo-mineral complexes due to a high specific surface area, thereby providing the chemical protection of SOC in clay soils (Oades, 1988; von Lutzow et al., 2006). The formed organo-mineral complexes can also increase organic matter hydrophobicity and reduce the availability of substrates and enzyme, thus preventing microorganisms from decomposing organic matter (Six et al., 2002; von Lutzow et al., 2006). Moreover, soil organic matter in the clay fraction is more recalcitrant, in contrast to the soil organic matter in the sand or silt fractions (Christensen, 2001; von Lutzow et al., 2006). Generally, organic matter was dominated by fragments of plant and microbial tissues (i.e. carbohydrates and protein C) in sand particles, by partially decomposed residue components (lignin and alkyl structures increased) in silt particles, and by recalcitrant chemical structures (i.e. alkyl C) in clay particles (Baldock and Skjemstad, 2000). Chen and Chiu (2003) indicated that the humification index (alkyl/*O*-alkyl-C) increased with decreasing soil particle-size. These results demonstrated an accumulation of recalcitrant organic matter in the fine particle-size fractions. Second, soil texture (particularly the soil clay content) can also influence the formation of soil aggregates (McLauchlan, 2006; von Lutzow et al., 2006). Generally, high concentrations of soil clay are associated with increased aggregation (particularly microaggregates) and the stability of aggregates (McLauchlan, 2006). Furthermore, with increased soil clay content, the proportion of small pores increases, which hinders the decomposition of SOC (Mtambanengwe et al., 2004). When organic C is occluded within aggregates, it is rendered inaccessible to soil microbes and their enzymes due to pore size exclusion, hence, it is physically protected from microbial decomposition (von Lutzow et al., 2006). Chenu and Stotzky (2002) indicated that most fungi were found

in the external spaces of aggregates. Mtambanengwe et al. (2004) also suggested that soil microorganisms mainly live in certain sized pores. Furthermore, these aggregates may also decrease the diffusion of oxygen and alter soil moisture, which can restrict aerobic decomposition (von Lutzow et al., 2006). According to the above discussion, in line with our study, increased clay content translated to lower SOC decomposition rate. Additionally, several studies put forward that the clay content regulated the decomposition of recalcitrant SOC pools only (McLauchlan, 2006; Wang et al., 2003). However, our results showed that the decomposition of active and slow C pools was mediated by the clay content. Although organic C were bound to clay particle surfaces, or occluded within aggregates assumed to be recalcitrant C, soil clay may influence soil moisture, oxygen availability, and microbial communities (McLauchlan, 2006; von Lutzow et al., 2006). Our study also demonstrated that soil clay content affected the C residence times through the regulation of soil qMB (Fig. 5). Therefore, the decomposition of both active and slow C pools was influenced by the clay content.

4.3. Effect of pH and C:N on C residence time

Another important factor that regulates the C residence time is soil pH, which directly influences SOC solubility or indirectly impacts soil microbial communities and activities (Rousk et al., 2009; Tavakkoli et al., 2015). In general, it is often assumed that the SOC decomposition rate is enhanced with higher soil pH of acidic soils (Malik et al., 2018; Marinos and Bernhardt, 2018). However, there are many inconsistent views as relates to the effects of soil pH on the SOC decomposition rate in neutral and alkaline soils (Ding et al., 2016b; Gonzalez-Dominguez et al., 2019; Xu et al., 2016). Our results indicated that increased soil pH (6.7–8.4) resulted in the amplification of the slow C pool decomposition rate. High soil pH enhances substrate availability due to the desorption of organic matter by reducing the binding force of clay (Tavakkoli et al., 2015; Zhang et al., 2018). Additionally, the organic C bound to clay particle surfaces was assumed to be recalcitrant C (Christensen, 2001; Jindaluang et al., 2013). Moreover, the activities of soil residing oxidative enzymes (i.e. peroxidase and phenol oxidase) associated with the decay of recalcitrant organic C were found to be higher in alkaline soils than other soils (Stursova and Sinsabaugh, 2008). Consequently, high soil pH might promote the decomposition of the slow C pool. It is generally accepted that soil pH is the dominant factor that influences soil microbial communities and activities, which, in turn, governs the decomposition of SOC (Rousk et al., 2009). However, our results revealed that there were no relationships between soil pH and microbial properties (Fig. S2), which may have been due to soil pH (6.7–8.4) being suitable for microbial activtiy. Blagodatskaya and Kuzyakov (2008) also suggested that microbial activity was higher with soil pH ranged from 6 to 8.

The soil C:N ratio might reflect the quality of soil organic matter, and thus control microbial activity, while influencing the SOC decomposition and C residence times (Chen et al., 2016b). Generally, the C:N ratio is positively correlated with the C residence time (Xu et al., 2016). High soil C:N ratios indicate the low N availability, which leads to the reduced SOC decomposition (Xu et al., 2016). Our findings are partly consistent with previous studies, as our results indicated only that the soil C:N ratio was positively correlated with the slow C pool residence time. Most of the organic matter was the recalcitrant C matter pool, particularly at our study sites, where > 90% of the C pool was slow and passive (Table 4). Accordingly, the C:N ratio cannot actually represent the C:N ratio of the active C pool. Huang et al. (2011) indicated that there was almost no difference between soil C:N ratio and heavy fraction (recalcitrant) C:N ratio, however, there was a significant difference between the C:N ratio and light fraction (labile) C:N ratio.

5. Conclusions

This study demonstrated that the data assimilation approach could accurately estimate the residence times of active and slow C pools based on the time-series data of soil incubation experiments. Our results revealed that (1) the RT_A increased with the clay content and significantly decreased with qMB; (2) the RT_S significantly increased with clay content and C:N ratio, but significantly decreased with soil pH and qMB; and (3) the determinants of RT_A and RT_S were different, as qMB was more important for the RT_A, while soil pH was the most important regulator of the RT_S. Our findings improve our understanding of terrestrial C dynamics, and are essential to accurately predict future C-climate feedbacks on the Tibetan Plateau.

Acknowledgments

We are grateful to Professor Dafeng Hui from Tennessee State University for improving the language. This study was funded by the Open Project Program of Key Laboratory of Education Ministry on Environment and Ecology in Tibetan Plateau (2018-QHS-K07), National Key Research and Development Program of China (2016YFC0500505), Natural Science Foundation of China (31502010; 31870434; 41671106), Key Scientific and Technological Projects of Xinjiang (2016A03006-1), Open Project Program of State Key Laboratory of Grassland Agro-ecosystems (SKLGAE201401) and the China Scholarship Council.

Appendix A. Supplementary data

Supplementary data to this article can be found online at https://doi.org/10.1016/j.geoderma.2019.113942.

References

Alef, K., 1995. Soil respiration. In: Alef, K., Nannipieri, P. (Eds.), Methods in Applied Soil Microbiology and Biochemistry. Acadamic Press, London, pp. 214–222.
Anav, A., Friedlingstein, P., Kidston, M., Bopp, L., Ciais, P., Cox, P., Jones, C., Jung, M., Myneni, R., Zhu, Z., 2013. Evaluating the land and ocean components of the global carbon cycle in the CMIP5 earth system models. J. Clim. 26 (18), 6801–6843.
Arai, H., Hadi, A., Darung, U., Limin, S.H., Takahashi, H., Hatano, R., Inubushi, K., 2014. Land use change affects microbial biomass and fluxes of carbon dioxide and nitrous oxide in tropical peatlands. Soil Sci. Plant Nutr. 60 (3), 423–434.
Baldock, J.A., Skjemstad, J.O., 2000. Role of the soil matrix and minerals in protecting natural organic materials against biological attack. Org. Geochem. 31 (7–6), 697–710.
Baumann, F., He, J.S., Schmidt, K., Kühn, P., Scholten, T., 2009. Pedogenesis, permafrost, and soil moisture as controlling factors for soil nitrogen and carbon contents across the Tibetan Plateau. Glob. Chang. Biol. 15 (12), 3001–3017.
Blagodatskaya, E., Kuzyakov, Y., 2008. Mechanisms of real and apparent priming effects and their dependence on soil microbial biomass and community structure: critical review. Biol. Fertil. Soils 45 (2), 115–131.
Bremner, J., 1996. Nitrogen-total. In: Sparks, D., Page, A., Helmke, P., Loeppert, R., Soltanpour, P., Tabatabai, M., Johnston, C., Sumner, M. (Eds.), Methods of Soil Analysis. Part 3-chemical Methods. Soil Science Society of America, Madison, WI, pp. 1085–1121.
Brookes, P.C., Landman, A., Pruden, G., Jenkinson, D.S., 1985. Chloroform fumigation and the release of soil-nitrogen - a rapid direct extraction method to measure microbial biomass nitrogen in soil. Soil Biol. Biochem. 17 (6), 837–842.
Chen, J.S., Chiu, C.Y., 2003. Characterization of soil organic matter in different particle-size fractions in humid subalpine soils by CP/MAS 13C NMR. Geoderma 117 (1–2), 129–141.
Chen, Y.Z., Xia, J.Y., Sun, Z.G., Li, J.L., Luo, Y.Q., Gang, C.C., Wang, Z.Q., 2015. The role of residence time in diagnostic models of global carbon storage capacity: model decomposition based on a traceable scheme. Sci. Rep. 5.
Chen, J., Zhou, X., Wang, J., Hruska, T., Shi, W., Cao, J., Zhang, B., Xu, G., Chen, Y., Luo, Y., 2016a. Grazing exclusion reduced soil respiration but increased its temperature sensitivity in a Meadow Grassland on the Tibetan Plateau. Ecol. Evol. 6 (3), 675–687.
Chen, L., Liang, J., Qin, S., Liu, L., Fang, K., Xu, Y., Ding, J., Li, F., Luo, Y., Yang, Y., 2016b. Determinants of carbon release from the active layer and permafrost deposits on the Tibetan Plateau. Nat. Commun. 7, 1–12.
Chenu, C., Stotzky, G., 2002. Interactions between microorganisms and soil particles: an overview. In: Huang, P.M., Bollage, J.-M., Senesi, N. (Eds.), Interactions Between Soil Particles and Microorganisms: Impact on the Terrestrial Ecosystem. John Wiley and Sons, West Sussex, England, pp. 3–39.
Christensen, B.T., 2001. Physical fractionation of soil and structural and functional complexity in organic matter turnover. Eur. J. Soil Sci. 52 (3), 345–353.
Deng, Q., Cheng, X.L., Hui, D.F., Zhang, Q., Li, M., Zhang, Q.F., 2016. Soil microbial community and its interaction with soil carbon and nitrogen dynamics following afforestation in central China. Sci. Total Environ. 541, 230–237.

Derrien, D., Amelung, W., 2011. Computing the mean residence time of soil carbon fractions using stable isotopes: impacts of the model framework. Eur. J. Soil Sci. 62 (2), 237–252.
Ding, J., Li, F., Yang, G., Chen, L., Zhang, B., Liu, L., Fang, K., Qin, S., Chen, Y., Peng, Y., Ji, C., He, H., Smith, P., Yang, Y., 2016a. The permafrost carbon inventory on the Tibetan Plateau: a new evaluation using deep sediment cores. Glob. Chang. Biol. 22 (8), 2688–2701.
Ding, J.Z., Chen, L.Y., Zhang, B.B., Liu, L., Yang, G.B., Fang, K., Chen, Y.L., Li, F., Kou, D., Ji, C.J., Luo, Y.Q., Yang, Y.H., 2016b. Linking temperature sensitivity of soil CO_2 release to substrate, environmental, and microbial properties across alpine ecosystems. Glob. Biogeochem. Cycles 30 (9), 1310–1323.
FAO, 2006. Guidelines for soil description, Fourth ed. Food and Agriculture Organisation of the United States, Rome.
Giardina, C.P., Ryan, M.G., Hubbard, R.M., Binkley, D., 2001. Tree species and soil textural controls on carbon and nitrogen mineralization rates. Soil Sci. Soc. Am. J. 65 (4), 1272–1279.
Gonzalez-Dominguez, B., Niklaus, P.A., Studer, M.S., Hagedorn, F., Wacker, L., Haghipour, N., Zimmermann, S., Walther, L., McIntyre, C., Abiven, S., 2019. Temperature and moisture are minor drivers of regional-scale soil organic carbon dynamics. Sci. Rep. 9.
Gregorich, E.G., Beare, M.H., 2008. Physically uncomplexed organic matter. In: M.R. Carter, E.G. Gregorich (Eds.), Soil Sampling and Methods of Analysis (second ed.). CRC Press, Boca Raton, FL, pp. 607–616.
Guo, D., Wang, J., Fu, H., Wen, H.Y., Luo, Y.Q., 2017. Cropland has higher soil carbon residence time than grassland in the subsurface layer on the Loess Plateau, China. Soil Tillage Res. 174, 130–138.
Hastings, W.K., 1970. Monte Carlo sampling methods using Markov chains and their applications. Biometrika 57 (1), 97–109.
He, Y., Trumbore, S.E., Torn, M.S., Harden, J.W., Vaugh, L.J.S., Allison, S.D., Randerson, J.T., 2016. Radiocarbon constraints imply reduced carbon uptake by soils during the 21st century. Science 353 (6306), 1419–1424.
Holland, E.A., Neff, J.C., Townsend, A.R., McKeown, B., 2000. Uncertainties in the temperature sensitivity of decomposition in tropical and subtropical ecosystems: implications for models. Glob. Biogeochem. Cycles 14 (4), 1137–1151.
Huang, Z., Davis, M.R., Condron, L.M., Clinton, P.W., 2011. Soil carbon pools, plant biomarkers and mean carbon residence time after afforestation of grassland with three tree species. Soil Biol. Biochem. 43 (6), 1341–1349.
Jindaluang, W., Kheoruenromne, I., Suddhiprakarn, A., Singh, B.P., Singh, B., 2013. Influence of soil texture and mineralogy on organic matter content and composition in physically separated fractions soils of Thailand. Geoderma 195, 207–219.
Lagomarsino, A., Benedetti, A., Marinari, S., Pompili, L., Moscatelli, M.C., Roggero, P.P., Lai, R., Ledda, L., Grego, S., 2011. Soil organic C variability and microbial functions in a Mediterranean agro-forest ecosystem. Biol. Fertil. Soils 47 (3), 283–291.
Landgraf, D., Klose, S., 2002. Mobile and readily available C and N fractions and their relationship to microbial biomass and selected enzyme activities in a sandy soil under different management systems. J. Plant Nutr. Soil Sci. 165 (1), 9–16.
Landgraf, D., Wedig, S., Klose, S., 2005. Medium- and short-term available organic matter, microbial biomass, and enzyme activities in soils under Pinus sylvestris L. and Robinia pseudoacacia L. in a sandy soil in NE Saxony, Germany. J. Plant Nutr. Soil Sci. 168 (2), 193–201.
Liao, M., Xie, X.M., Peng, Y., Ma, A.L., 2011. Changes of soil microbiological characteristics after Solidago canadensis L. invasion. Agric. Sci. China 10 (7), 1064–1071.
Liu, X., Chen, B., 2000. Climatic warming in the Tibetan Plateau during recent decades. Int. J. Climatol. 20 (14), 1729–1742.
Liu, Y.Z., Zhou, T., Crowley, D., Li, L.Q., Liu, D.W., Zheng, J.W., Yu, X.Y., Pan, G.X., Hussain, Q., Zhang, X.H., Zheng, J.F., 2012. Decline in topsoil microbial quotient, fungal abundance and C utilization efficiency of rice paddies under heavy metal pollution across South China. PLoS One 7 (6).
Luo, Y.Q., Weng, E.S., Wu, X.W., Gao, C., Zhou, X.H., Zhang, L., 2009. Parameter identifiability, constraint, and equifinality in data assimilation with ecosystem models. Ecol. Appl. 19 (3), 571–574.
Luo, Y.Q., Ahlstrom, A., Allison, S.D., Batjes, N.H., Brovkin, V., Carvalhais, N., Chappell, A., Ciais, P., Davidson, E.A., Finzi, A.C., Georgiou, K., Guenet, B., Hararuk, O., Harden, J.W., He, Y.J., Hopkins, F., Jiang, L.F., Koven, C., Jackson, R.B., Jones, C.D., Lara, M.J., Liang, J.Y., McGuire, A.D., Parton, W., Peng, C.H., Randerson, J.T., Salazar, A., Sierra, C.A., Smith, M.J., Tian, H.Q., Todd-Brown, K.E.O., Torn, M., van Groenigen, K.J., Wang, Y.P., West, T.O., Wei, Y.X., Wieder, W.R., Xia, J.Y., Xu, X., Xu, X.F., Zhou, T., 2016. Toward more realistic projections of soil carbon dynamics by Earth system models. Glob. Biogeochem. Cycles 30 (1), 40–56.
Malik, A.A., Puissant, J., Buckeridge, K.M., Goodall, T., Jehmlich, N., Chowdhury, S., Gweon, H.S., Peyton, J.M., Mason, K.E., van Agtmaal, M., Blaud, A., Clark, I.M., Whitaker, J., Pywell, R.F., Ostle, N., Gleixner, G., Griffiths, R.I., 2018. Land use driven change in soil pH affects microbial carbon cycling processes. Nat. Commun. 9.
Marinos, R.E., Bernhardt, E.S., 2018. Soil carbon losses due to higher pH offset vegetation gains due to calcium enrichment in an acid mitigation experiment. Ecology 99 (10), 2363–2373.
McLauchlan, K.K., 2006. Effects of soil texture on soil carbon and nitrogen dynamics after cessation of agriculture. Geoderma 136 (1–2), 289–299.
Metropolis, N., Rosenbluth, A.W., Rosenbluth, M.N., Teller, A.H., Teller, E., 1953. Equation of state calculations by fast computing machines. J. Chem. Phys. 21, 1087.
Mtambanengwe, F., Mapfumo, P., Kirchmann, H., 2004. Decomposition of organic matter in soil as influenced by texture and pore size distribution. In: Bationa, A. (Ed.), Managing Nutrient Cycles to Sustain Soil Fertility in Sub-Saharan Africa. Academy Science Publishers and TSBF CIAT, Nairobi, Kenya, pp. 261–275.
Nelson, D.W., Sommers, L.E., 1996. Total carbon, organic carbon, and organic matter. In: Sparks, D., Page, A., Helmke, P., Loeppert, R., Soltanpour, P., Tabatabai, M., Johnston, C., Sumner, M. (Eds.), Methods of Soil Analysis. Part 3-chemical Methods. Soil Science Society of America, Madison, WI, pp. 961–1010.
Oades, J.M., 1988. The retention of organic-matter in soils. Biogeochemistry 5 (1), 35–70.
Pajares, S., Gallardo, J.F., Masciandaro, G., Ceccanti, B., Marinari, S., Etchevers, J.D., 2009. Biochemical indicators of carbon dynamic in an Acrisol cultivated under different management practices in the central Mexican highlands. Soil Tillage Res. 105 (1), 156–163.
Parton, W.J., Schimel, D.S., Cole, C.V., Ojima, D.S., 1987. Analysis of factors controlling soil organic-matter levels in Great-Plains grasslands. Soil Sci. Soc. Am. J. 51 (5), 1173–1179.
Paterson, E., Osler, G., Dawson, L.A., Gebbing, T., Sim, A., Ord, B., 2008. Labile and recalcitrant plant fractions are utilised by distinct microbial communities in soil: independent of the presence of roots and mycorrhizal fungi. Soil Biol. Biochem. 40 (5), 1103–1113.
Percival, H.J., Parfitt, R.L., Scott, N.A., 2000. Factors controlling soil carbon levels in New Zealand grasslands: is clay content important? Soil Sci. Soc. Am. J. 64 (5), 1623–1630.
Plante, A.F., Conant, R.T., Stewart, C.E., Paustian, K., Six, J., 2006. Impact of soil texture on the distribution of soil organic matter in physical and chemical fractions. Soil Sci. Soc. Am. J. 70 (1), 287–296.
Rousk, J., Brookes, P.C., Bååth, E., 2009. Contrasting soil pH effects on fungal and bacterial growth suggest functional redundancy in carbon mineralization. Appl. Environ. Microbiol. 75 (6), 1589–1596.
Schädel, C., Luo, Y., Evans, R.D., Fei, S., Schaeffer, S.M., 2013. Separating soil CO_2 efflux into C-pool-specific decay rates via inverse analysis of soil incubation data. Oecologia 1–12.
Schädel, C., Schuur, E.A., Bracho, R., Elberling, B., Knoblauch, C., Lee, H., Luo, Y., Shaver, G.R., Turetsky, M.R., 2014. Circumpolar assessment of permafrost C quality and its vulnerability over time using long-term incubation data. Glob. Chang. Biol. 20 (2), 641–652.
Serna-Chavez, H.M., Fierer, N., van Bodegom, P.M., 2013. Global drivers and patterns of microbial abundance in soil. Glob. Ecol. Biogeogr. 22 (10), 1162–1172.
Six, J., Conant, R.T., Paul, E.A., Paustian, K., 2002. Stabilization mechanisms of soil organic matter: implications for C-saturation of soils. Plant Soil 241 (2), 155–176.
Sparling, G.P., 1992. Ratio of microbial biomass carbon to soil organic-carbon as a sensitive indicator of changes in soil organic-matter. Aust. J. Soil Res. 30 (2), 195–207.
Stursova, M., Sinsabaugh, R.L., 2008. Stabilization of oxidative enzymes in desert soil may limit organic matter accumulation. Soil Biol. Biochem. 40 (2), 550–553.
Tavakkoli, E., Rengasamy, P., Smith, E., McDonald, G.K., 2015. The effect of cation-anion interactions on soil pH and solubility of organic carbon. Eur. J. Soil Sci. 66 (6), 1054–1062.
Todd-Brown, K.E.O., Randerson, J.T., Post, W.M., Hoffman, F.M., Tarnocai, C., Schuur, E.A.G., Allison, S.D., 2013. Causes of variation in soil carbon simulations from CMIP5 Earth system models and comparison with observations. Biogeosciences 10 (3), 1717–1736.
Todd-Brown, K.E.O., Randerson, J.T., Hopkins, F., Arora, V., Hajima, T., Jones, C., Shevliakova, E., Tjiputra, J., Volodin, E., Wu, T., Zhang, Q., Allison, S.D., 2014. Changes in soil organic carbon storage predicted by Earth system models during the 21st century. Biogeosciences 11 (8), 2341–2356.
Trumbore, S.E., 1997. Potential responses of soil organic carbon to global environmental change. Proc. Natl. Acad. Sci. U. S. A. 94 (16), 8284–8291.
Vance, E.D., Brookes, P.C., Jenkinson, D.S., 1987. An extraction method for measuring soil microbial biomass-C. Soil Biol. Biochem. 19 (6), 703–707.
von Lutzow, M., Kogel-Knabner, I., Ekschmitt, K., Matzner, E., Guggenberger, G., Marschner, B., Flessa, H., 2006. Stabilization of organic matter in temperate soils: mechanisms and their relevance under different soil conditions - a review. Eur. J. Soil Sci. 57 (4), 426–445.
Wagner, S., Cattle, S.R., Scholten, T., 2007. Soil-aggregate formation as influenced by clay content and organic-matter amendment. J. Plant Nutr. Soil Sci. 170 (1), 173–180.
Wang, G., Qian, J., Cheng, G., Lai, Y., 2002. Soil organic carbon pool of grassland soils on the Qinghai-Tibetan Plateau and its global implication. Sci. Total Environ. 291 (1–3), 207–217.
Wang, W.J., Dalal, R.C., Moody, P.W., Smith, C.J., 2003. Relationships of soil respiration to microbial biomass, substrate availability and clay content. Soil Biol. Biochem. 35 (2), 273–284.
Wang, X.L., Jia, Y., Li, X.G., Long, R.J., Ma, Q.F., Li, F.M., Song, Y.J., 2009. Effects of land use on soil total and light fraction organic, and microbial biomass C and N in a semi-arid ecosystem of northwest China. Geoderma 153 (1–2), 285–290.
Wang, J., Sun, J., Xia, J., He, N., Li, M., Niu, S., 2018. Soil and vegetation carbon turnover times from tropical to boreal forests. Funct. Ecol. 32 (1), 71–82.
Wei, Y.A., Yu, L.F., Zhang, J.C., Yu, Y.C., Deangelis, D.L., 2011. Relationship between vegetation restoration and soil microbial characteristics in degraded karst regions: a case study. Pedosphere 21 (1), 132–138.
Wen, L., Lei, P., Xiang, W., Yan, W., Liu, S., 2014. Soil microbial biomass carbon and nitrogen in pure and mixed stands of Pinus massoniana and Cinnamomum camphora differing in stand age. For. Ecol. Manag. 328, 150–158.
Xu, T., White, L., Hui, D.F., Luo, Y.Q., 2006. Probabilistic inversion of a terrestrial ecosystem model: analysis of uncertainty in parameter estimation and model prediction. Glob. Biogeochem. Cycles 20 (2), 1–15.
Xu, X., Shi, Z., Li, D., Rey, A., Ruan, H., Craine, J.M., Liang, J., Zhou, J., Luo, Y., 2016. Soil properties control decomposition of soil organic carbon: results from data-assimilation analysis. Geoderma 262, 235–242.
Yang, Y., Fang, J., Tang, Y., Ji, C., Zheng, C., He, J., Zhu, B., 2008. Storage, patterns and controls of soil organic carbon in the Tibetan grasslands. Glob. Chang. Biol. 14 (7), 1592–1599.
Yang, Y., Ji, C., Chen, L., Ding, J., Cheng, X., Robinson, D., 2015. Edaphic rather than

climatic controls over < sup > 13 < /sup > C enrichment between soil and vegetation in alpine grasslands on the Tibetan Plateau. Funct. Ecol. 29 (6), 839–848.
Yu, S.Y., He, H.L., Cheng, P., Hou, Z.F., 2017. Depth heterogeneity of soil organic carbon dynamics in a heavily grazed alpine meadow on the northeastern Tibetan Plateau: a radiocarbon-based approach. J. Geophys. Res. Biogeosci. 122 (7), 1775–1788.
Zhang, L., Luo, Y.Q., Yu, G.R., Zhang, L.M., 2010. Estimated carbon residence times in three forest ecosystems of eastern China: applications of probabilistic inversion. J. Geophys. Res. Biogeosci. 115, G01010.
Zhang, H., Wu, P., Fan, M., Zheng, S., Wu, J., Yang, X., Zhang, M., Yin, A., Gao, C., 2018. Dynamics and driving factors of the organic carbon fractions in agricultural land reclaimed from coastal wetlands in eastern China. Ecol. Indic. 89, 639–647.
Zhao, L., Chen, D.D., Zhao, N., Li, Q., Cheng, Q., Luo, C.Y., Xu, S.X., Wang, S.P., Zhao, X.Q., 2015. Responses of carbon transfer, partitioning, and residence time to land use in the plant-soil system of an alpine meadow on the Qinghai-Tibetan Plateau. Biol. Fertil. Soils 51 (7), 781–790.
Zhou, X., Zhou, T., Luo, Y., 2012. Uncertainties in carbon residence time and NPP-driven carbon uptake in terrestrial ecosystems of the conterminous USA: a Bayesian approach. Tellus B 64 (1), 17223.